Drink. Water Eng. Sci., 10, 109–117, 2017
https://doi.org/10.5194/dwes-10-109-2017

Drinking Water
Engineering and Science
Open Access

Photocatalytic degradation of dyes in water by analytical reagent grades ZnO, TiO_2 and SnO_2: a comparative study

Dnyaneshwar R. Shinde, Popat S. Tambade, Manohar G. Chaskar, and Kisan M. Gadave

Prof. Ramkrishna More Arts, Commerce and Science College, Akurdi,
Pune-44, affiliated with Savitribai Phule Pune University, Pune, India

Correspondence to: Popat S. Tambade (pstam3@rediffmail.com)

Received: 20 May 2017 – Discussion started: 2 June 2017
Revised: 29 September 2017 – Accepted: 6 October 2017 – Published: 16 November 2017

Abstract. In this study, we evaluated the photocatalytic activities of analytical reagent (AR) grade ZnO, TiO_2, and SnO_2 to identify a low-cost photocatalyst for dye degradation. The obtained samples of ZnO, TiO_2, and SnO_2 were characterised by X-ray diffractogram (XRD), scanning electron microscope imaging, and UV-VIS diffuse reflectance spectroscopy. The decolourisation of three structurally diverse dyes, namely crystal violet, basic blue, and methyl red under solar irradiation, was used to evaluate the photocatalytic activities of three metal oxides. The photocatalytic activities of the received three metal oxides were tested with the photocatalytic degradation of dyes and compared with Degussa P-25. Dye solutions with each metal oxide at initial pH 9 were subjected to irradiation under sunlight and monitored for up to the stage of complete decolourisation. The results indicate that ZnO exhibited the highest photocatalytic activity as compared to TiO_2 and SnO_2 as well as that of Degussa P-25 (TiO_2). The photocatalytic dye decolourisation rates with ZnO were 1.14–1.35, 1.70–3.1, and 4–8.5 times higher than those of the Degussa P-25, TiO_2, and SnO_2, respectively. The percentage COD removal was studied for ZnO and partial removal was observed at the decolourisation stage. To enhance photocatalytic activity of AR grade ZnO, it was loaded with Ag metal and about 20 % enhancement in the activity was observed.

1 Introduction

Dyes and pigments are extensively used in industries that manufacture and process textiles, paper, plastics, leather, food, and cosmetic products. The release of dye-containing effluents from these industries into water bodies poses a considerable threat to aquatic life as well as the environment. Numerous studies have investigated the efficient removal of hazardous organic molecules from waste water during past decades. These studies have demonstrated that the hazardous organic molecules in waste water can be degraded using photo excited charge carriers in an excited semiconductor (Yang et al., 2001; Qi et al., 2014; Singh et al., 2015; Wang et al., 2016; Keane et al., 2014; Shinde et al., 2015). This process is termed photocatalysis. The most suitable natural energy source for semiconductor-based photocatalysis is solar irradiation (Nguyen et al., 2015). However, solar irradiation can be optimally used for photocatalysis only by designing an efficient solar-irradiation-driven photocatalytic system. Recently, many semiconductors, such as SnO_2, WO_3, TiO_2, CeO_2, and ZnO, have been used in heterogeneous photocatalysis (Xu et al., 2013; Herrmann, 1999). Most of these semiconductors are wide-band-gap semiconductors, which require ultraviolet (UV) irradiation for photocatalysis (Lin and Lin, 2007; Abo et al., 2016). When a wide-band-gap photocatalyst is irradiated with light of energy equal to or higher than its band-gap energy, electron–hole pairs are created. In an aqueous medium, reactants may be adsorbed on the surface of a photocatalyst and may react directly or indirectly with the photo-generated electrons and holes (Girish Kumar and Koteswara Rao, 2015; Nagaraja et al., 2012). Photocatalysis was reported to enable efficient degradation of a wide range of organic pollutants and hazardous inorganic materials into readily biodegradable compounds, and eventually mineralise them into relatively harmless CO_2 and water (Chong et al., 2010). In the category of semiconductor photocatalysts TiO_2 and ZnO have been widely investigated

(Pardeshi and Patil, 2008; Parida and Parija, 2006). TiO_2 is generally considered to be a non-toxic, chemically inert, and photo-stable catalyst, and it has the ability to degrade dyes as well as several organic pollutants (Hu et al., 2013; Zhou et al., 2011; Akpan and Hameed, 2009). The Degussa P-25 photocatalyst (mixture of anatase and rutile TiO_2) exhibited significantly higher photocatalytic activity in organic dye degradation than do other commercially used forms of TiO_2 (Lydakis-Simantiris et al., 2010; Zhou et al., 2012; Hou et al., 2015). The extensive use of TiO_2 for large-scale water treatment is uneconomical; therefore, studies to identify suitable alternatives to TiO_2 have been conducted worldwide. ZnO has been widely studied as a photocatalyst in water treatment because of its low cost and favourable optoelectronic and catalytic properties (Nagaraja et al., 2012). ZnO is an n-type semiconductor with many attractive features. It has a wide band gap of 3.2 eV and a large number of active sites. ZnO is an efficient visible-light photocatalyst and generates large quantities of hydroxyl radicals. Surface and core defects, such as oxygen vacancies, zinc interstitials, and oxygen interstitials, in ZnO play a vital role in the photocatalytic reactions by providing active sites for preventing electron–hole recombination (Han et al., 2012; Janotti and Van de Walle, 2009). This, in turn, enhances the generation of hydrogen peroxide (H_2O_2), superoxide (O_2^{-*}) radicals, and hydroxyl (OH^*) radicals, which have been reported to be responsible for the photocatalytic activity (Girish Kumar and Koteswara Rao, 2015), on the ZnO surface. Doping ZnO nanoparticles with metals and transition metals such as Ag, Pb, Mn, and Co can increase the photocatalytic activity because doping increases surface defects (Patil et al., 2010; Sood et al., 2014; Zhi-gang et al., 2012).

We systematically studied the photocatalytic activity of commercially available analytical reagent (AR) grade ZnO, TiO_2, and SnO_2 powders during the degradation of industrial dyes, namely crystal violet (CV), basic blue (BB), and methyl red (MR) in aqueous solutions under solar irradiation. Furthermore, the activities of these photocatalysts were compared with that of the Degussa P-25 photocatalyst. Dye degradation studies were performed in a specially designed reactor called the flat slurry reactor (FSR). We expect that this work will provide crucial theoretical insights and will have practical applications in the treatment of polluted water that results from the widespread disposal of organic pollutants.

2 Experimental methods

2.1 Materials

The Degussa P-25 photocatalyst was obtained from Nanoshel (US) (characteristic information: in Table S1 in the Supplement) and used as a benchmark photocatalyst. Commercially available AR grade TiO_2, ZnO_2, and SnO_2 were purchased from Loba Chemie Ltd. (India). Three structurally diverse dyes, namely crystal violet (CV), methyl red (MR), and basic blue (BB), used in this investigation were purchased from Sigma-Aldrich (India) (Table S2). All the materials were used without further purification. Tap water was used for preparation of dye solutions, and the pH of the solutions was adjusted using 1 M NaOH or 1 M H_2SO_4.

2.2 Characterisation of photocatalysts

The powder X-ray diffractograms (XRDs) of the as-received ZnO, TiO_2, and SnO_2 samples were recorded and analysed to determine their crystal structure and lattice parameters. The average particle size of each metal oxide was estimated using the Debye–Scherrer formula. The band gaps were evaluated from diffuse reflectance spectra (DRS) of metal oxides in absorbance mode. Particle morphology was analysed through scanning electron microscopic (SEM) imaging. Specific surface areas were calculated using a prescribed method (Jiji et al., 2006; Jo-Yong et al., 2006).

2.3 Photoreactor and degradation experiment

Photocatalytic experiments were carried out in a specially designed FSR. The reactor consisted of a rectangular reaction vessel of size $20 \times 30 \times 4\,cm^3$. The reaction vessel was connected to a stirring tank (volume 300 mL) through polyethylene pipes of 10 mm diameter (Fig. 1). The reaction mixture was collected from the reaction vessel into a stirring tank, stirred, and pumped back into the reaction vessel. The reaction mixture was stirred and circulated continuously to maintain the catalyst in the form of a suspension. The experiments were performed using solar irradiation incident between 10:00 and 15:00, where the intensity of the irradiation was 57 000–66 000 lx.

The reaction conditions such as pH, catalyst dose, stirring rate, and circulation rate of the reaction mixture were optimised in preliminary experiments and a reaction was performed under optimised experimental conditions. Except for pH and temperature, all other parameters remained constant during the experiment. The pH of the dye solution was decreased from 9 ± 0.1 to 8.6 ± 1, while temperature raised from room temperature to $39 \pm 3\,^{\circ}C$. Each dye solution ($10\,mg\,L^{-1}$) was prepared using tap water. To 2000 mL of dye solution, $400\,mg\,L^{-1}$ photocatalyst was added and a suspension was developed by stirring. The suspension was placed in the dark for 1 h to achieve the adsorption–desorption equilibrium before exposure to solar irradiation. Then 1.2 L suspension was transferred to the reactor and exposed to solar irradiation. The same procedure was used for all the catalysts used in the study. The photocatalytic activity of each metal oxide was determined under optimised conditions of the pH of the dye solution ($pH = 9$). At predetermined time intervals, 10 mL of each reaction mixture was withdrawn and centrifuged, and the absorbance of supernatant was determined at λ_{max} of the dye at a specified

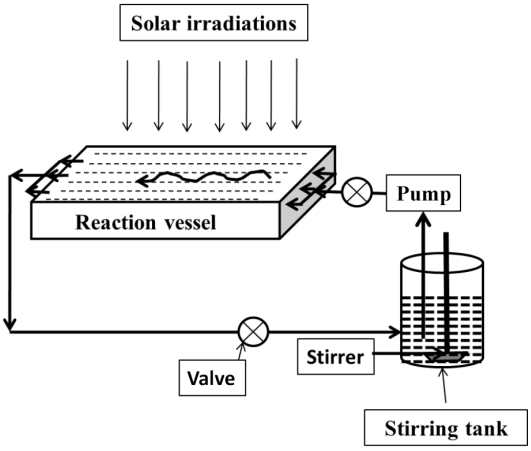

Figure 1. Reactor set-up for photodegradation of dye under solar irradiation.

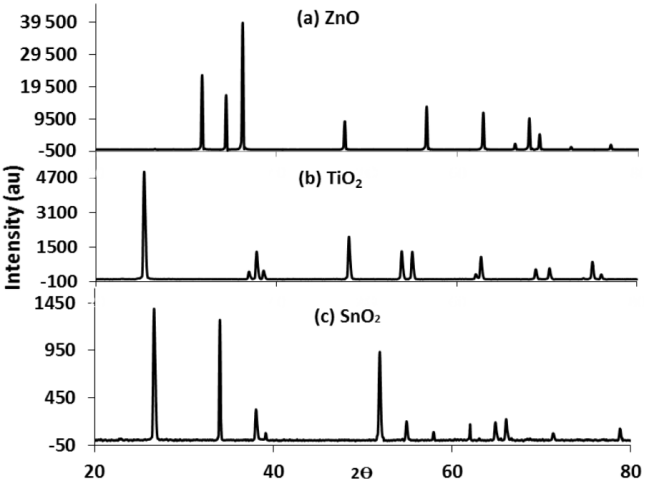

Figure 2. XRDs of **(a)** ZnO, **(b)** TiO_2, and **(c)** SnO_2.

pH. The rate constant of the decolourisation reaction was determined using the Langmuir–Hinshelwood equation (Chong et al., 2009):

$$k_{\text{obs}} = \frac{2.303}{t} \log_{10}\left(\frac{A_0}{A}\right), \quad (1)$$

where k_{obs} is the apparent reaction rate constant, A_0 is the initial absorbance of the dye solution, and A is the absorbance of the dye solution after irradiation at time t.

Finally, we have determined a decrease in the chemical oxygen demand (COD) of a treated dye solution according to the previously described method (Pawar et al., 2016).

2.4 Loading Ag metal on AR grade ZnO

Five grams of AR grade ZnO were sonicated for 5 min in 100 mL 0.01 M $AgNO_3$ solution, stirred for 30 min and centrifuged to recover ZnO. The recovered ZnO was suspended in an alkaline (using ammonia) glucose solution (0.1 M, 100 mL, pH = 9) and was boiled for 5 min. The ZnO was recovered through centrifugation; it was washed with distilled water until it was free from alkali. Finally, it was annealed for 30 min in a furnace at 450 °C.

3 Results and discussion

3.1 Characterisation of catalysts

Powder XRD analyses were conducted on the as-received AR grade ZnO, TiO_2, and SnO_2 to investigate their crystalline phases, lattice parameters, and average crystallite sizes. Figure 2 represents the XRDs of the three as-received semiconductor samples.

Figure 2a depicts the XRD patterns of ZnO. The major diffraction peaks are observed for ZnO at 2O angles 31.78, 34.44, 36.27, 47.55, 56.61, 62.87, 66.39, 67.96, and 69.10°, which are indexed to the planes [100], [002], [101], [102], [110], [103], [200], [112], and [201], respectively. These peaks match the hexagonal cubic (wurtzite) structure of ZnO (JCPDS 36-1451) (Pawar et al., 2016). In Fig. 2b, separate and sharp diffraction peaks of TiO_2 are observed at 25.3, 37.79, 48.04, 53.9, 55.07, 62.7, 68.78, 70.30, and 75.08°, corresponding to planes,[101], [004], [200], [105], [211], [213], [116], [220], and [215], respectively, of the pure anatase (tetragonal) phase of TiO_2 (JCPDS 21-1272). Figure 2c depicts the diffraction peaks of SnO_2 at 26.66, 34.03, 38.07, 39.15, 42.67, 51.93, 54.94, 57.96, 62.04, 64.88, 66.07, 71.34, and 78.81°, which can be indexed to the planes [100], 10 [101], [200], [111], [220], [211], [220], [002], [310], [112], [301], [202], and [321], respectively, of the rutile (cassiterite) crystalline phase of SnO_2 (JCPDS 77-0451) (Zhang et al., 2009; Elsayed et al., 2014).

Lattice parameters were calculated for all three metal oxides by using XRD data and are listed in Table 1. The lattice parameters were consistent with reported values (Pawar et al., 2016; Cheng et al., 2011; Li et al., 2014, 2013). Crystallite sizes were calculated using the intense peaks in XRD by the Debay–Sherrer formula; they were 103, 36, and 66 nm for ZnO, TiO_2, and SnO_2, respectively.

3.2 SEM micrographs of catalysts

Figure 3 presents typical SEM micrographs of the as-received catalysts. The SEM micrographs of metal oxides reveal the agglomeration of primary particles (crystallites) to form grains of larger sizes. Fewer ZnO crystallites were agglomerated into cubic grains, many into elongated hexagonal rods of various diameters. TiO_2 grains are roughly spherical with various diameters (range 55–170 nm). SnO_2 exhibits roughly spherical or irregular-shaped particles of sizes in the range 86–230 nm. The particles of all three oxides are small and have smooth surfaces.

Table 1. Unit cell parameters calculated from XRD data.

Parameters	ZnO	TiO_2	SnO_2
a (Å)	3.248	3.784	4.734
c (Å)	5.203	9.514	3.179
c/a ratio	1.602	2.514	0.672
Unit cell volume ($\times 10^{-23}$ cm^3)	4.756	13.62	7.125
X-ray density (g cm^{-3})	5.681	3.894	7.023

3.3 Band gaps of ZnO, TiO_2 and ZnO

The corresponding DRS in the absorbance mode of the as-received oxides, namely ZnO, TiO_2, and SnO_2, are provided in Fig. 4. These spectra indicate strong absorbance in the UV region and an absorption edge between 300 and 400 nm because of the relatively large excitation binding energy. The absorbance onsets of wurtzite ZnO, anatase TiO_2, and rutile SnO_2 are 384, 387, and 341 nm, respectively.

The experimentally evaluated band gaps of ZnO, TiO_2, and SnO_2 are 3.23, 3.20, and 3.64 eV, respectively (Fig. S1). The observed band gaps are strongly correlated with reported values (Cheng et al., 2013; Anand et al., 2008; Gupta and Tripathi, 2011). The band gap order of these three oxides is $TiO_2 \sim ZnO < SnO_2$.

3.4 Specific surface area of catalysts

The specific surface areas of AR grade ZnO, TiO_2, and SnO_2 powders were determined using a prescribed method. Among the three oxides, TiO_2 exhibited the highest specific surface area (42.54 m^2 g^{-1}) because of its relatively small particle size and low crystal density. ZnO and SnO_2 have comparable specific surface areas, 10.18 and 12.91 m^2 g^{-1}, respectively, which are approximately 4 times less than that of TiO_2. Such differences can be attributed to large crystallite sizes and high crystal densities of ZnO and SnO_2 compared with those of TiO_2. The specific surface area of the Degussa P-25 catalyst is approximately 50 m^2 g^{-1}.

3.5 Photocatalytic activity

To compare the photocatalytic activity of commercially available AR grade metal oxides, namely ZnO, TiO_2, and SnO_2, and P-25, a set of photocatalytic experiments were performed under similar conditions using the dyes CV, BB, and MR. In the present study we have utilised FSR, since it has a suitable design for an external source of irradiation like sunlight and is easy to operate. In preliminary experiments we have optimised process parameters affecting the rate of degradation of dyes. The parameters studied were initial pH of dye solution, catalyst dose, depth of dye solution in the reactor and the circulation rate. pH variation was performed over a limited range (5 to 9) as a very high or low pH is not desirable in water treatment. Depending

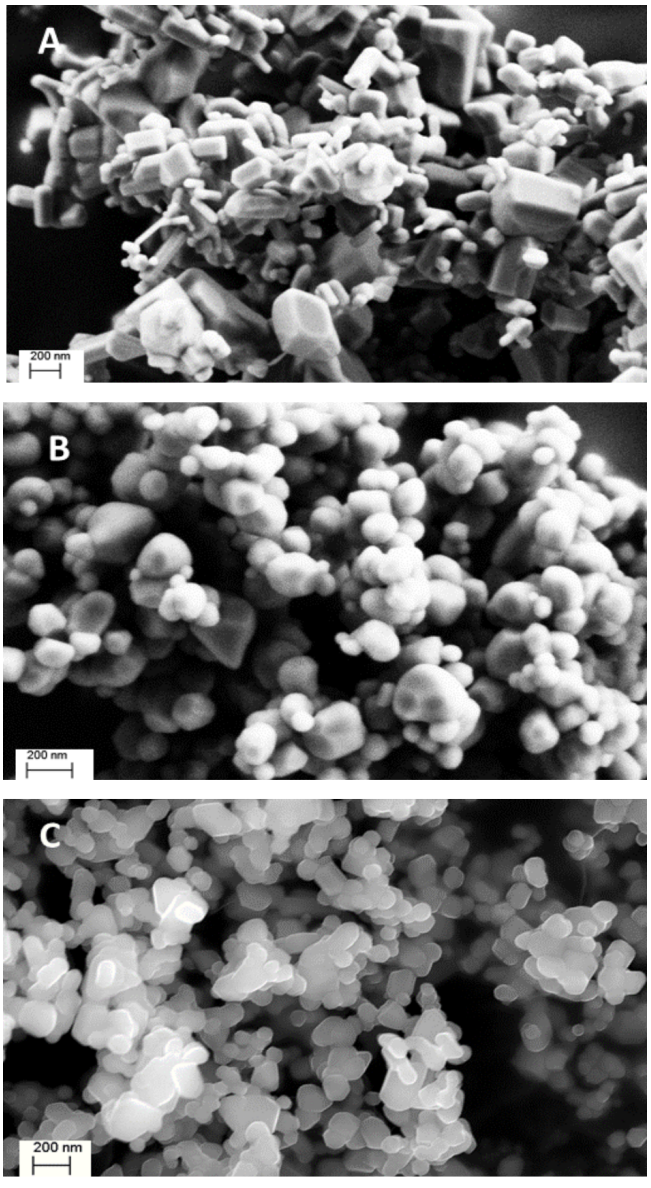

Figure 3. SEM micrographs of ZnO **(A)**, TiO_2 **(B)**, and SnO_2 **(C)**.

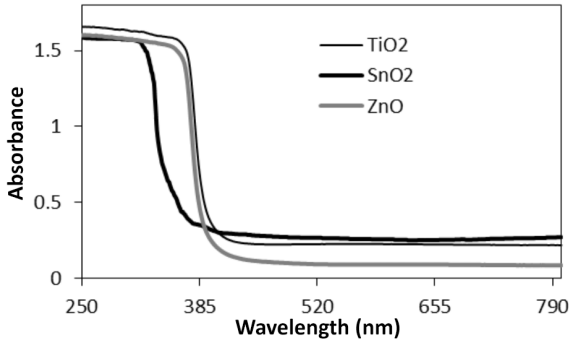

Figure 4. Diffuse absorbance spectra of ZnO, TiO_2, and SnO_2.

on the results of these experiments, we have selected process parameters in this study. The selected parameters were pH = 9, catalyst dose = 400 mg L^{-1}, depth of solution in reactor = 1.5 cm, and circulation rate = 130 mL min^{-1}. Control experiments were performed on the dye solutions for 3 h (i) under solar irradiation without a catalyst and (ii) in the dark with the addition of a catalyst. When dye solutions were irradiated with the light without catalyst loading, negligible decolourisation (less than 2 %) was observed. When the experiments were performed with catalyst loadings in the dark, 5–16 % decolourisation was observed for CV and BB, which could be attributed to the adsorption of these dyes on the catalyst surface (Table 2).

The photocatalytic activities were compared in terms of the rate constant of decolourisation of dyes, which were obtained using the graphical method (graph of $\log_{10}(A_0/A_t)$ against time; Fig. S2) on photocatalysts and are listed in Table 3.

The results indicate that for all three dyes, ZnO exhibited higher photocatalytic activity than did TiO_2, SnO_2, and P-25. Comparative studies on ZnO and TiO_2 (the Degussa P-25 TiO_2) photocatalysts have been performed by many other researchers, where synthetic ZnO has shown a higher performance than TiO_2 (Hussein and Abass, 2010; Sakthivel et al., 2003; Qamar and Muneer, 2009). Han et al. (2012) accounted for enhanced photocatalytic activity of ZnO in terms of higher absorbance of radiations by ZnO than by TiO_2 in the UV region. The surface area of a photocatalyst is one of the key parameters that affects photocatalytic activity. Among the four catalysts used in the study, ZnO displayed the lowest specific surface area, while the Degussa P-25 photocatalyst had the highest specific surface area. The results revealed that despite having a low specific surface area, ZnO exhibited a higher photocatalytic activity than did TiO_2 and SnO_2. This might be because of differences in the intrinsic characteristics of ZnO, TiO_2, and SnO_2. Quantum efficiency may be used to explain the differences in photocatalytic activity; ZnO has a greater quantum efficiency than do TiO_2 and SnO_2 (Kansal et al., 2007). Another critical factor affecting the photocatalytic activity is the band gap. In our study, SnO_2 exhibited a relatively low activity because of its wide band gap (3.64 eV). Since a wide band gap photocatalyst needs a large amount of UV radiation to excite electrons and to form electron–hole pairs in the catalyst (Sakthivel et al., 2003; Abo et al., 2016). ZnO and TiO_2 exhibited comparable band gaps (3.24 and 3.20 eV, respectively). The Degussa P-25 photocatalyst has the lowest band gap (3.00 eV) and was expected to exhibit a higher photocatalytic activity than ZnO. However, the experimental results clearly indicate that ZnO had a higher photocatalytic activity than did the Degussa P-25 photocatalyst and TiO_2. Solar irradiation consists of 5–7 % in the ultraviolet radiations. The results of the photocatalytic activities provide indirect evidence that ZnO may be able to absorb larger fractions of photon energy more efficiently than P-25 and TiO_2 within the UV region (Pardeshi and Patil, 2008). This behaviour may be attributed to the intrinsic defects in ZnO crystals. The predominant defects in the ZnO are positively charged Zn interstitials and oxygen vacancies. When electron–hole pairs are formed, the Zn interstitials and oxygen vacancies facilitate redox reactions by trapping photo-generated electrons. This reduces the recombination of electrons and holes, and they are available for dye degradation (Han et al., 2012). The Degussa P-25 photocatalyst is a blend of rutile (30 %) and anatase (70 %) TiO_2, which prevents the recombination of electrons and holes; therefore, it shows more photocatalytic activity than does anatase TiO_2.

Table 2. Percent decolourisation (adsorption) of three dyes on photocatalysts in the dark.

Photocatalyst	Percent decolourisation		
	CV	BB	MR
ZnO	9.8 ± 1.2	16.3 ± 0.8	negligible
TiO_2	5.3 ± 0.7	8.4 ± 1.1	negligible
SnO_2	4.6 ± 0.8	7.4 ± 0.4	negligible
Degussa	6.9 ± 0.6	7.4 ± 0.6	negligible

Dye degradation by photocatalyst under solar irradiation takes place through two different mechanisms. In the first mechanism, when the photocatalyst is illuminated, a photon of energy higher than or equal to the band gap causes excitation of electrons into the conduction band (CB) of the photocatalyst. Simultaneously, an equal number of holes are generated in the valence band (VB). The high oxidative potential of the hole in the CB of catalyst permits the direct oxidation of the dye to reactive intermediates followed by degradation. The process is expressed as in Reactions (R1) to (R5) (Konstantinou and Albanis, 2004)

$$\mathrm{MO/MO_2} + h\nu \rightarrow \mathrm{MO/MO_2}\left(e^-_{\mathrm{CB}} + h^+_{\mathrm{VB}}\right), \quad \text{(R1)}$$

$$h^+_{\mathrm{VB}} + \mathrm{dye} \rightarrow \mathrm{dye}* \rightarrow \text{dye degradation}. \quad \text{(R2)}$$

The degeneration of dyes also occurs due to their reaction with hydroxyl ($OH^\bullet$) and superoxide ($O_2^{-\bullet}$) free radicals. $OH^\bullet$ is a highly reactive, strong oxidising chemical species, which is either formed through decomposition of water or by the reaction of a hole with surface-bound hydroxyl groups (OH^-):

$$h^+_{\mathrm{VB}} + \mathrm{H_2O} \rightarrow \mathrm{H^+} + \mathrm{OH^\bullet}, \quad \text{(R3)}$$

$$h^+_{\mathrm{VB}} + \mathrm{OH^-} \rightarrow \mathrm{OH^\bullet}. \quad \text{(R4)}$$

The conduction band (e^-_{CB}) potential was sufficiently negative to reduce O_2, which is adsorbed on the surface of the catalyst to generate $O_2^{-\bullet}$:

$$e^-_{\mathrm{CB}} + \mathrm{O_2} \rightarrow \mathrm{O_2}^{\bullet-}. \quad \text{(R5)}$$

The subsequent reactions of OH^- and $O_2^{\bullet-}$ can also generate $OH^\bullet$. The reactions of $OH^\bullet$ and $O_2^{\bullet-}$ with dye molecules degrade them into simple molecules (Chen and Ray, 2001). The

Table 3. Comparison of photocatalytic activities in terms of reaction rate constants for three dyes.

Photocatalyst	CV		BB		MR	
	k (min^{-1})	$t_{1/2}$ (min)	k (min^{-1})	$t_{1/2}$ (min)	k (min^{-1})	$t_{1/2}$ (min)
ZnO	0.079	8.8	0.10	6.9	0.014	49.6
TiO_2	0.026	26.9	0.045	15.5	0.008	84.1
SnO_2	0.010	71.0	0.017	40.7	0.004	196.7
P 25	0.060	11.6	0.076	9.1	0.012	56.4

second mechanism is a dye sensitisation mechanism. In this mechanism, the dye molecules adsorbed on the surface of the catalyst absorb visible radiations and undergo electronic excitation from the highest occupied molecular orbitals to the lowest unoccupied molecular orbitals (LUMO). Then excited electrons from the LUMO of the dye molecule are injected into the conduction band (CB) of the photocatalyst and the dye is converted into a cationic dye radical (Lakshmi Prasanna and Rajagopalan, 2016). This dye radical undergoes degradation to produce mineralised products (Li et al., 2002; Muthirulan et al., 2013). The electron in the CB of the metal oxide is further scavenged by oxygen to produce $O_2^{\bullet-}$ and results in the decolourisation of dyes. This mechanism is prominent when dye molecules are in an adsorbed state on the catalyst surface. These two mechanisms are depicted in Fig. 5.

The adsorption study of dyes in solution by photocatalysts showed that CV and BB were adsorbed to a certain extent on all four photocatalysts, while MR was adsorbed to a negligible extent (Table 2).

The quantity of adsorption was clearly reflected in terms of the decolourisation rate constants of these dyes. When rate constants (Table 3) are compared with percentage adsorption (Table 2), it is observed that MR has the lowest rate constant, which might be due to negligible adsorption. Furthermore, BB is adsorbed to a greater extent than CV; thereby, it showed greater decolourisation rates with all four catalysts. This supports the dye sensitised mechanism.

3.6 Enhancement of photocatalytic activity of AR grade ZnO

To broaden the photo response of ZnO catalyst for the solar spectrum, various material engineering approaches have been devised. These approaches include doping (with metals, non-metals or metalloids), composition with carbon nanotubes, formation of hetero-structures with noble metals or other semiconductors, and dye sensitisers (Zhang and Zeng, 2010). In this study, we attempted to enhance the photocatalytic activity of commercially available ZnO by loading silver metal on its surface. The ZnO was suspended in an $AgNO_3$ solution, where it adsorbed Ag^+ ions on its surface (adsorbed quantity 1.9 mg g^{-1} ZnO). When the ZnO with adsorbed Ag^+ was treated with an alkaline glucose solution, the Ag^+ was reduced to Ag metal according to the following chemical reaction (Eq. 7).

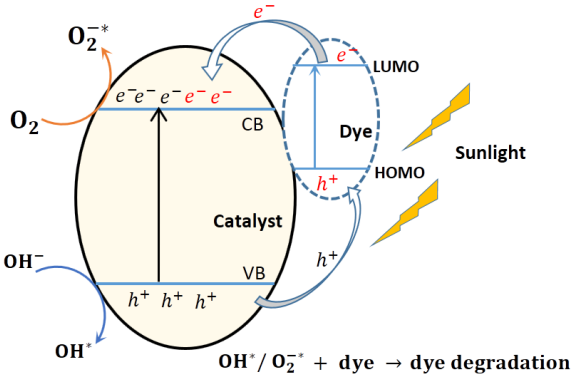

Figure 5. Schematics of photodegradation of dye in solar irradiation.

$$Ag^+ + C_6H_{12}O_6 \xrightarrow{NH_4OH,\ \Delta} Ag_{metal} + C_6H_{12}O_7 \quad \text{(R6)}$$

The presence of Ag metal on the surface was clearly indicated by the appearance of a light-grey colour to the surface-sensitised ZnO. The Ag-sensitised ZnO was characterised by powder XRD, which showed extra peaks at $2O = 38.1$, 44.3, 64.5, and 77.9° in addition to hexagonal wurtzite peaks of ZnO (Fig. S3). These peaks were characteristic of face-centred cubic crystallised Ag metal (JCDS data file no. 04-0783) (Ma et al., 2014). Relatively small peak intensities corresponding to Ag metal indicate its smaller crystal size on the surface of ZnO. The presence of Ag metal was also confirmed through DRS in absorbance mode and energy-dispersive X-ray spectroscopy (Figs. S4 and S5).

The process of photocatalysis by Ag/ZnO is depicted in Fig. 6. The coupling of Ag metal with ZnO alters the band structure of the photocatalyst. The CB energy of Ag metal is lower than that of ZnO. Molecules of the dyes that adhered to the ZnO particle surface are excited by the incoming light and release electrons from the LUMO to the CB of ZnO. The ZnO is also excited by the UV component of solar irradiation, thus forming electron–hole pairs, and the electrons are available in the CB of ZnO. Eventually, these electrons are

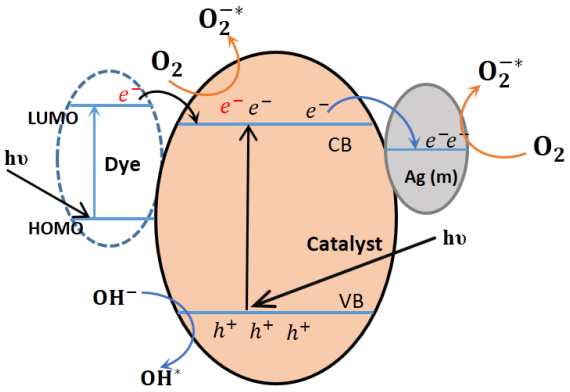

Figure 6. Schematic diagram representing the band structure silver metal loaded ZnO, electronic excitation process, dye sensitised mechanism and electron delocalisation in silver metal loaded ZnO.

transported to the CB of the Ag metal. This delocalisation of the electrons is thermodynamically favourable and facilitates reduction of the rate of recombination of electron–hole pairs produced during the photo-excitation of ZnO. In turn, more electrons and holes are made available for chemical reactions, which enhance the photocatalytic activity of Ag-loaded ZnO (Kuriakose et al., 2014; Jing et al., 2006). These electrons and holes are responsible for the generation of O_2^{-*} and $OH^\bullet$ free radicals, respectively, which are extremely strong oxidants for the decomposition of dyes.

The calculated rate constant for decolourisation of MR, CV and BB using the Ag-loaded ZnO is 1.22, 1.28 and 1.33 times higher, respectively, than that of pure ZnO. These results indicate that the loading of Ag on ZnO enhances the photocatalytic activity of ZnO in solar irradiation. Ag deposits on ZnO surfaces have been reported to act as electron sinks and hinder the recombination of photo-induced electrons and holes. This ensures that the charge separation on Ag-loaded ZnO is higher than that on ZnO. The charge-transfer process occurring at the Ag–ZnO interface assists the transport of electrons to the surface, which is responsible for enhancing photocatalytic activity (Patil et al., 2016; Zheng et al., 2008). Dinesh et al. (2014) demonstrated that the hybrid ZnO@Ag core–shell nano rods exhibit more effective degradation of rhodamine 6G, Congo red, and amido black B-10 than ZnO nano rods.

3.7 COD removal

In this study, we have estimated COD removal of a treated dye solution with AR grade ZnO as it showed higher photocatalytic activity. The results showed that a partial COD removal occurred at decolourisation stages of dyes (46 % for CV, 53 % for BB and 38 % for MR). To achieve further COD removal, the experiment was continued up to 5 h. Analysis of the results indicated that COD removal is not significantly different at 4 and 5 h irradiation time. At the end of 5 h irradiation time, observed COD removal was 92 % for CV, 95 % for BB and 89 % for MR (Table S3).

3.8 Cost comparison

The suitability of a particular photocatalyst during the photocatalytic removal of organic pollutants in the water depends on its activity and cost. ZnO, TiO_2, and SnO_2 cost INR 1100 = 00, 2800 = 00, and 8000 = 00, per kg, respectively, while the cost of Degusa P-25 is INR 120 000 = 00 per kg. A comparison of costs reveals that AR grade ZnO is less expensive (and hence is affordable) than are Degussa P-25 or AR grade TiO_2 and SnO_2. Even after accounting for the cost of starting material and other chemicals, labour, time, special requirements of equipment, and electricity consumed, any laboratory-synthesised form of ZnO, TiO_2, and SnO_2 will remain costlier than the commercially available AR metal oxides. In brief, AR grade ZnO is a cost-effective and efficient material for the photocatalytic degradation of organic dyes under solar irradiation in an aqueous medium.

4 Conclusion

Photocatalysis based on metal oxide semiconductors is an important approach to the utilisation of the abundant energy from the sun for dye degradation. Intense research efforts have led to significant progress for the complete mineralisation of organic pollutants using nanomaterial like ZnO, TiO_2, and SnO_2 under light illumination. In the present study, the authors have compared photocatalytic activity of ZnO, TiO_2, SnO_2 and Degussa P-25 in the degradation of industrial dyes (CV, BB, and MR) under optimised conditions of pH (pH 9), catalyst dose (400 mg L^{-1}), depth of dye solution (1.5 cm) and rate of circulation (130 mL min^{-1}) and identical conditions of sunlight intensity and dye concentration. A comparison of the photocatalytic activity of ZnO with the benchmark, the Degussa P-25 (TiO_2), as well as with AR grade TiO_2 and SnO_2, showed that despite low specific surface area and relatively large grain size, ZnO displayed higher photocatalytic activity in the degradation of dyes (CV, BB, and MR) under solar irradiation. The photocatalytic activity of AR grade ZnO can be enhanced by coupling it with a noble metal such as Ag. The cost of AR grade ZnO is lower than that of the other photocatalyst used in this study. Therefore, we suggest that solar photocatalysis using AR grade ZnO can prove to be cost effective and an energy efficient method.

Data availability. The research data of this work can be obtained by contacting the corresponding author.

The Supplement related to this article is available online at https://doi.org/10.5194/dwes-10-109-2017-supplement.

Competing interests. The authors declare that they have no conflict of interest.

Acknowledgements. The authors thank the Pune District Education Association, Pune, for providing partial financial support to the research work of this article.

Edited by: Ran Shang
Reviewed by: two anonymous referees

References

Abo, R., Kummer, N.-A., and Merkel, B. J.: Optimized photodegradation of Bisphenol A in water using ZnO, TiO_2 and SnO_2 photocatalysts under UV radiation as a decontamination procedure, Drink. Water Eng. Sci., 9, 27–35, https://doi.org/10.5194/dwes-9-27-2016, 2016.

Akpan, U. G. and Hameed, B. H.: Parameters affecting the photocatalytic degradation of dyes using TiO_2based photocatalysts: A review, J. Hazard. Mater., 170, 520–529, 2009.

Anand, M., Shim, H.-S., Kim, Y. S., and Kim, W. B.: Structural and Optical Properties of Co- and Ti-ZnO Composite Nanofibers Prepared by Using an Electrospinning Method, J. Korean Phys. Soc., 53, 2423–2426, 2008.

Chen, D. and Ray, A. K.: Removal of toxic metal ions from wastewater by semiconductor photocatalysis, Chem. Eng. Sci., 56, 1561–1570, 2001.

Cheng, G., Chen, J., Ke, H., Shang, J., and Chu, R.: Synthesis, characterization and photocatalysis of SnO_2nanorods with large aspect ratios, Mater. Lett., 65, 3327–3329, 2011.

Cheng, G., Hao, T., Ke, H., Gong, F., Chen, J., and Shang, J.: Controlled growth of SnO_2 nanostructures with small diameters 5 and their photocatalytic properties, IET Micro. Nano. Lett., 8, 473–475, 2013.

Chong, M. N., Jin, B., Chow, C. W. K., and Saint, C. P.: A new approach to optimize an annular slurry reactor system for the degradation of Congo-red: Statistical analysis and modelling, Chem. Eng. J., 152, 158–166, 2009.

Chong, M. N., Jin, B., Chow, C. W. K., and Saint, C.: Recent developments in photocatalytic water treatment technology: A review, Water Res., 44, 2997–3027, 2010.

Dinesh, V. P., Biji, P., Ashok, A., Dhara, S. K., Kamruddin, M., Tyagi, A. K., and Raj, B.: Plasmon-mediated, highly enhanced photocatalytic degradation of industrial textile dyes using hybrid ZnO@Ag core–shell nanorods, RSC Adv., 4, 58930–58940, 2014.

Elsayed, E. M., Shalan, A. E., and Rashad, M. M.: Preparation of ZnO nanoparticles using electrodeposition and co-precipitation techniques for dye-sensitized solar cells applications, J. Mater. Sci.-Mater. El., 25, 3412–3419, 2014.

Girish Kumar, S. and Koteswara Rao, K. S. R.: Zinc oxide based photocatalysis: tailoring surface bulk structure and related interfacial charge carrier dynamics for better environmental applications, RSC Adv., 5, 3306–3351, 2015.

Gupta, S. M. and Tripathi, M.: A review of TiO_2 nanoparticles, Chinese Sci. Bull., 56, 1639–1657, https://doi.org/10.1007/s11434-011-4476-1, 2011.

Han, J., Liu, Y., Singhal, N., Wang, L., and Gao, W.: Comparative photocatalytic degradation of estrone in water by ZnO and TiO_2 under artificial UV-A and solar irradiation, Chem. Eng. J., 213, 150–162, 2012.

Herrmann, J. M.: Heterogeneous photocatalysis: fundamentals and applications to the removal of various types of aqueous pollutants, Catal. Today, 53, 115–129, 1999.

Hou, H., Shang, M., Wang, L., Li, W., Tang, B., and Yang, W.: Efficient Photocatalytic Activities of TiO_2 Hollow Fibers with Mixed Phases and Mesoporous Walls, Sci. Rep., 5, 15228, https://doi.org/10.1038/srep15228, 2015.

Hu, A., Liang, R., Zhang, X., Kurdi, S., Luong, D., Huang, H., Peng, P., Marzbanrad, E., Oakes, K. D., Zhou, Y., and Servos, M. R.: Enhanced photocatalytic degradation of dyes by TiO_2nanobelts with hierarchical structures, J. Photoch. Photobio. A, 256, 7–15, 2013.

Hussein, F. H. and Abass, T. A.: Photocatalytic treatment of textile industrial wastewater, Int. J. Chem. Sci., 8, 1353–1364, 2010.

Janotti, A. and Van de Walle, C. G.: Fundamentals of zinc oxide as a semiconductor, Rep. Prog. Phys., 72, 126501–126529, 2009.

Jiji, A., Joseph, N., Donald, R. B., Daniel, M., Amit, S., and Qiang, Y.: Size-Dependent Specific Surface Area of Nanoporous Film Assembled by Core-Shell Iron Nanoclusters, J. Nanomater., 2006, 54961, https://doi.org/10.1155/JNM/2006/54961, 2006.

Jing, L. Q., Qu, Y., Wang, B., Li, S., Jiang, B., Yang, L., Wei, F., and Fu, H.: Review of photoluminescence performance of nan0-sized semiconductor materials and its relationship with photocatalytic activity, J. Sol. Energ. Mat. Sol. C., 90, 1773–1787, 2006.

Jo-Yong, P., Yun-Jo, L., Ki-Won, J., Jin-Ook B. G., and Dae, J. Y.: Chemical Synthesis and Characterization of Highly Oil Dispersed MgO Nanoparticles, J. Ind. Eng. Chem., 12, 882–887, 2006.

Kansal, S. K., Singh, M., and Sud, D.: Studies on photodegradation of two commercial dyes in aqueous phase using different photocatalysts, J. Hazard. Mater., 141, 581–590, 2007.

Keane, D. A., McGuigan, K. G., Ibáñez, P. F., Polo-López, M. I., Byrne, J. A., Dunlop, P. S. M., O'Shea, K., Dionysioufg, D. D., and Pillai, S. C.: Solar photocatalysis for water disinfection: materials and reactor design, Catal. Sci. Technol., 4, 1211–1226, 2014.

Konstantinou, I. K. and Albanis, T. A.: TiO_2-assisted photocatalytic degradation of azo dyes in aqueous solution: Kinetic and mechanistic investigations. A review, Appl. Catal. B-Environ., 49, 1–14, 2004.

Kuriakose, S., Choudhary, V., Satpati, B., and Mohapatra, S.: Enhanced photocatalytic activity of Ag–ZnO hybrid plasmonic nanostructures prepared by a facile wet chemical method, Beilstein J. Nanotechnol., 5, 639–650, https://doi.org/10.3762/bjnano.5.75, 2014.

Lakshmi Prasanna, V. and Rajagopalan, V.: A New Synergetic Nanocomposite for Dye Degradation in Dark and Light, Sci. Rep., 6, 38606, https://doi.org/10.1038/srep38606, 2016.

Li, K., Xiong, J., Chen, T., Yan, L., Dai, Y., Song, D., Lv, Y., and Zeng, Z.: Preparation of graphene/TiO_2 composites by nonionic surfactant strategy and their simulated sunlight and visible light photocatalytic activity towards representative aqueous POPs degradation, J. Hazard. Mater., 250–251, 19–28, 2013.

Li, X. Z., Zhao, W., and Zhao, J. C.: Visible light-sensitized semiconductor photocatalytic degradation of 2,4-dichlorophenol, Sci. China Ser. B, 45, 421–425, 2002.

Li, Y., Qin, Z., Guo, H., Yang, H., Zhang, G., Ji, S., and Zeng, T.: Low-Temperature Synthesis of Anatase TiO_2 Nanoparticles with Tunable Surface Charges for Enhancing Photocatalytic Activity, PLoS ONE, 9, 114638, https://doi.org/10.1371/journal.pone.0114638, 2014.

Lin, C. and Lin, K.: Photocatalytic oxidation of toxic organohalides with TiO_2/UV: The effects of humic substances and organic mixtures, Chemosphere, 66, 1872–1877, 2007.

Lydakis-Simantiris, N., Riga, D., Katsivela, E., Mantzavinos, D., and Xekoukoulotakis, N. P.: Disinfection of spring water and secondary treated municipal wastewater by TiO_2 photocatalysis, Desalination, 250, 351–355, 2010.

Ma, S., Xue, J., Zhou, Y., and Zhang, Z.: Photochemical synthesis of ZnO/Ag_2O heterostructures with enhanced ultraviolet and visible photocatalytic activity, J. Mater. Chem. A, 2, 7272–7278, 2014.

Muthirulan, P., Meenakshisundararam, M., and Kannan, N.: Beneficial role of ZnO photocatalyst supported with porous activated carbon for the mineralization of alizarin cyanin green dye in aqueous solution, J. Adv. Res., 4, 479–484, 2013.

Nagaraja, R., Kottam, N., Girija, C. R., and Nagabhushana, B. M.: Photocatalytic degradation of Rhodamine B dye under UV/solar light using ZnO nanopowder synthesized by solution combustion route, Powder Technol., 215–216, 91–97, 2012.

Nguyen, C. C., Vu, N. N., and Do, T.: Recent advances in the development of sunlight driven hollow structure photocatalysts and their applications, J. Mater. Chem. A, 3, 18345–18359, 2015.

Pardeshi, S. K. and Patil, A. B.: A simple route for photocatalytic degradation of phenol in aqueous zinc oxide suspension using solar energy, Sol. Energy, 82, 700–705, 2008.

Parida, K. M. and Parija, S.: Photocatalytic degradation of phenol under solar radiation using microwave irradiated zinc oxide, Sol. Energy, 80, 1048–1054, 2006.

Patil, A. B., Patil, K. R., and Pardeshi, S. K.: Ecofriendly synthesis and solar photocatalytic activity of S-doped ZnO, J. Hazard. Mater., 183, 315–323, 2010.

Patil, S. S., Mali, M. G., Tamboli, M. S., Patil, D. R., Kulkarni, M. V., Yoon, H., Kim, H., Al-Deyab, S. S., Yoon, S. S., Kolekar, S. S., and Kale, B. B.: Green approach for hierarchical nanostructured Ag-ZnO and theirphotocatalytic performance under sunlight, Catal. Today, 260, 126–134, 2016.

Pawar, R. A., Shinde, D. R., and Tambade, P. S.: Synthesis of ZnO photocatalyst via ZnO_2 precursor and its application for dye degradation from effluent under solar irradiation, Desalination Water Treat., 57, 16514–16521, 2016.

Qamar, M. and Muneer, M.: A comparative activity of titanium oxide and zinc oxide by investigating the degradation of vanillin, Desalination, 249, 535–540, 2009.

Qi, L., Yu, J., Liu, G., and Wong, P. K.: Synthesis and photocatalytic activity of plasmonicAg@AgCl composite immobilized on titanate nanowire films, Catal. Today, 224, 193–199, 2014.

Sakthivel, S., Neppolian, B., Shankar, B. V., Arabindoo, B., Palanichamy, M., and Murugesan, V.: Solar photocatalytic degradation of azo dye: comparison of photocatalytic efficiency of ZnO and TiO_2, Sol. Energ. Mat. Sol. C., 77, 65–82, 2003.

Shinde, D. R., Qureashi, I., Pawar, R. A., and Pawar, R. R.: Enhancement of photocatalytic activity of ZnO via Nd(III) doping towards the degradation of dyes under solar irradiation, J. Nanoeng. Nanomanufact., 5, 197–203, 2015.

Singh, N. K., Saha, S., and Pal, A.: Solar light-induced photocatalytic degradation of methyl red in an aqueous suspension of commercial ZnO: a green approach, Desalination Water Treat., 53, 501–514, 2015.

Sood, S., Mehta, S. K., Umar, A., and Kansal, S. K.: The visible light-driven photocatalytic degradation of Alizarin red S using 30 Bi-doped TiO_2 nanoparticles, New J. Chem., 38, 3127–3136, 2014.

Wang, C., Zhang, Y., Zhu, T., Wang, P., and Gao, S.: Photocatalytic degradation of methylene blue and methyl orange in a Zn(II)-based Metal–Organic Framework, Desalination Water Treat., 57, 17844–17851, 2016.

Xu, L., Wei, B., Liu, W., Zhang, H,, Su, C., and Che, J.: Flower-like ZnO-Ag_2O composites: precipitation synthesis and photocatalytic activity, Nano. Res. Lett., 8, 536–541, 2013.

Yang, S., Tian, H., Xiao, H., Shang, X., Gong, X., Yao, S., and Chen, K.: Photodegradation of cyanine and merocyanine dyes, Dyes Pigments, 49, 93–101, 2001.

Zhang, D. and Zeng, F.: Synthesis of an Ag–ZnO nanocomposite catalyst for visible light-assisted degradation of a textile dye 5 in aqueous solution, Res. Chem. Intermed., 36, 1055–1063, 2010.

Zhang, Y., Wu, L., Xie, E., Duan, H., Han, W., and Zhao, J.: A simple method to prepare uniform-size nanoparticle TiO_2 electrodes for dye-sensitized solar cells, J. Power Sources, 189, 1256–1263, 2009.

Zheng, Y. H., Chen, C. Q., Zhan, Y. Y., Lin, X. Y., Zheng, Q., Wei, K. M., and Zhu, J. F.: Photocatalytic activity of Ag/ZnO heterostructure nano-catalyst: Correlation between structure and property, J. Phys. Chem. C, 112, 10773–10777, 2008.

Zhi-gang, J., Kuan-kuan, P., Yan-hua, L., and Rong-sun, Z.: Preparation and photocatalytic performance of porous ZnO microrods loaded with Ag, T. Nonferr. Metal. Soc., 22, 873–878, 2012.

Zhou, W., Du, G., Hu, P., Li, G., Wang, D., Liu, H., Wang, J., Boughton, R., Liu, D., and Jiang, H.: Nanoheterostructures on TiO_2 nanobelts achieved by acid hydrothermal method with enhanced photocatalyic and gas sensitive performance, J. Mater. Chem., 21, 7937–7945, 2011.

Zhou, X. T., Ji, H. B., and Huang, X. J.: Photocatalytic degradation of methyl orange over metalloporphyrins supported on TiO_2 degussa P25, Molecules, 17, 1149–1158, 2012.